Published in final edited form as:
Arterioscler Thromb Vasc Biol. 2011 August ; 31(8): 1908–1915. doi:10.1161/ATVBAHA.111.225268.

Imaging the Endothelial Glycocalyx *In Vitro* by Rapid Freezing/ Freeze Substitution Transmission Electron Microscopy

Eno E Ebong, Ph.D.[1,2,*], **Frank P Macaluso, M.Sc**[3], **David C Spray, Ph.D.**[2], and **John M Tarbell, Ph.D.**[1]

[1]Department of Biomedical Engineering, The City College of New York New York, NY, 10031

[2]Department of Neuroscience, Albert Einstein College of Medicine Bronx, NY, 10461

[3]Analytical Imaging Facility, Albert Einstein College of Medicine Bronx, NY, 10461

Abstract

Objective—Recent publications questioned the validity of endothelial cell (EC) culture studies of glycocalyx (GCX) function, due to findings that GCX *in vitro* may be substantially thinner than *in vivo*. The assessment of thickness differences is complicated by GCX collapse during dehydration for traditional electron microscopy. We measured *in vitro* GCX thickness using rapid freezing/ freeze substitution transmission electron microscopy (RF/FS-TEM), taking advantage of high spatial resolution provided by TEM and the capability to stably preserve the GCX in its hydrated configuration by RF/FS.

Methods and Results—Bovine aortic and rat fat pad endothelial cells (BAEC and RFPEC) were subjected to conventional- or RF/FS-TEM. Conventionally preserved BAEC GCX was ~0.040 μm in thickness. RF/FS-TEM revealed impressively thick BAEC GCX of ~11 μm and RFPEC GCX of ~5 μm. RF/FS-TEM also discerned GCX structure and thickness variations due to heparinase III enzyme treatment and extracellular protein removal, respectively. Immunoconfocal studies confirmed that the *in vitro* GCX is several microns thick and is comprised of extensive and well integrated heparan sulfate, hyaluronic acid, and protein layers.

Conclusions—New observations by RF/FS-TEM reveal substantial GCX layers on cultured EC, supporting their continued use for fundamental studies of GCX and its function in the vasculature.

Keywords

endothelium; glycocalyx; TEM; rapid freezing/freeze substitution; confocal microscopy

INTRODUCTION

The endothelial cell (EC) glycocalyx (GCX) senses the force (shear stress) of flowing blood and transmits it throughout the cell to sites where force is transduced into biochemical responses (mechanotransduction). Much of the evidence to support a role for the GCX and the mechanisms of its involvement in mechanotransduction comes from experiments in

*Address for correspondence: Department of Neuroscience Albert Einstein College of Medicine 1300 Morris Park Avenue, K840 Bronx, NY 10461 Tel: (718) 430-2570 Fax: (718) 430-8594 eno.ebong@einstein.yu.edu .

DISCLOSURES None.

which cultured EC have been treated with enzymes to selectively degrade specific components of the GCX prior to assessment of cell function. Such experiments have shown that the GCX mediates the shear-induced production of nitric oxide (NO)[1, 2], a central process in cardiovascular control, and that the NO-dependent shear-induced increases in endothelial layer hydraulic conductivity also rely on the GCX[3]. Related experiments have also revealed that the characteristic remodeling of the EC cytoskeleton and intercellular junctions in response to shear stress are GCX-dependent[4], as are EC elongation and alignment in the direction of shear[5].

The validity of using cell culture experiments to study EC GCX involvement in mechanotransduction and other physiological and pathophysiological processes has recently been questioned, due to findings that on average the thickness of the GCX *in vitro*[4, 6-13] may be drastically less than GCX thickness *in vivo*[7, 8, 12, 14-20] depending on the method of GCX assessment (Table 1). A major difficulty limiting the demonstration of the extent of an *in vitro* EC GCX has been a result of the decreased water content caused by the process of alcohol dehydration that follows fixation in preparation for electron microscopic visualization. While immunofluorescence confocal microscopy studies in which dehydration artifacts were suppressed revealed a glycocalyx of substantial thickness on cultured endothelial cells[4, 6, 9], spatial resolution of confocal microscopy is limited to several tenths of a micron and glare from fluorescent labels further affects the resolution.

We report on the application of rapid freezing/freeze substitution transmission electron microscopy (RF/FS-TEM) to assess GCX thickness and structure, taking advantage of the high spatial resolution provided by TEM, while avoiding the dehydration artifacts of conventional processing that usually accompany TEM. We tested the hypothesis that RF/FS-TEM GCX thickness is significantly greater than conventional TEM GCX thickness using TEM examination of bovine aortic endothelial cells (BAEC) fixed both conventionally and by quick freezing at liquid nitrogen temperatures, as performed and reported by Dalen et al.[21] and von Schack et al.[22] In quick frozen cells, the GCX was preserved in vitrified water (non-crystalline glassy ice)[23] and the vitrified water was subsequently exchanged for acetone through a process called freeze substitution, permitting the GCX and other hydrophilic cellular structures to remain configured as if alive.

We also assessed the utility of RF/FS-TEM for detecting differences in the GCX depending on cell type and on changes in environmental conditions. BAEC macrovascular GCX was compared to rat fat pad endothelial cell (RFPEC) microvascular GCX after both cell types were processed by RF/FS-TEM. BAEC and RFPEC were chosen for several reasons. BAEC are the most widely used and, therefore important, *in vitro* model for studies of fluid shear stress effects on EC. We have published GCX studies with BAEC[1-3] and much of what is known about EC response to shear stress was established in BAEC. We have also used RFPEC for studies of the role of the GCX in EC remodeling to shear stress[4]. In addition to comparing two different cell types, some EC were cultured in the presence of heparinase III at a concentration that selectively removes about 50% of the heparan sulfate component of the glycocalyx[2] and others were cultured in the absence of serum protein and bovine serum albumin (BSA) because Adamson and Clough[24] reported that insufficient protein in the endothelial environment leads to GCX collapse. We found that RF/FS-TEM enabled *in vitro* stabilization of the GCX (including its heparan sulfate component) in its hydrated and protein-rich configuration and observation of a surface layer of significant thickness that has never before been reported. This method clearly discerned thickness differences between the GCX of cells of different origin and a dramatically altered GCX structure or reduced thickness due to changing the culture environment.

Taken together, our findings suggest that EC cultures are appropriate for fundamental studies of GCX function in the vasculature. RF/FS-TEM fills a critical gap in the current state of the art in GCX research.

METHODS

Cell Culture

BAEC and RFPEC were cultured as previously described[2, 4]. Briefly, BAEC were harvested from bovine thoracic aortas or obtained from VEC Technologies (Rensselaer, NY). Whenever possible, experiments were conducted using both sets of BAEC and little difference in cell morphology and function were noted. RFPEC were cloned from cells isolated from capillaries of rat epididymal fat pads[25, 26]. Cells were grown at 37°C and 5% CO_2 in tissue culture flasks in MEM (BAEC) or DMEM (RFPEC) complete with supplements including 10% fetal bovine serum (FBS). Prior to experimentation, BAEC and RFPEC were seeded onto glass slides (Corning) (30 μg/mL fibronectin-coated for BAEC) at a cell density of 4×10^4 cells/cm^2 and allowed to grow to confluency for 2-3 days. For experimentation, the 10% FBS in the growth media was exchanged for 5% FBS and 0.5% bovine serum albumin (BSA) to sustain the GCX[4]. Some control samples were maintained for 2 hours prior to experimentation in media containing *F. heparinum* heparinase III (15 mU/mL, Sigma) to selectively remove about 50% of the fluorescence associated with the heparan sulfate GCX component[2]. Other control samples were cultured for 2 hours before experimentation in media with FBS and BSA removed to collapse the GCX[24].

Conventional- and RF/FS-TEM

EC GCX was labeled and examined by conventional TEM as previously described[15]. Briefly, EC were fixed for 1 hour in 2.0% paraformaldehyde and 2.5% glutaraldehyde containing 0.075% ruthenium red, 75 mM lysine, and 0.1 M cacodylate pH 7.2 and then fixed in the same solution with lysine removed. The ruthenium red component of the fixative solution binds to the GCX glycosaminoglycans. Following a rinse with 0.1 M cacodylate alone, cells were post-fixed with 1% osmium tetroxide to enhance contrast between cellular components, dehydrated through a graded series of ethanol solutions, and embedded in LX112 Resin.

For most of our GCX studies, RF/FS was used to preserve cell samples. The purpose of using this method was to limit GCX dehydration, damage, collapse, and loss of ultrastructure. For RF/FS-TEM, cells were quick frozen in a Life Cell CF 100 slam freezer by impacting the cell monolayer against a polished sapphire surface cooled to liquid nitrogen temperature. Frozen cells were transferred to a FS7500 Freeze Substitution Unit (RMC Inc. Tucson AZ) where they were freeze substituted in acetone containing 1% osmium tetroxide, thereby stabilizing the GCX while enhancing contrast to visualize of the GCX. They were stored at −90°C for 3 days then slowly raised to room temperature over 2-3 days, rinsed in acetone and embedded in LX112 Resin.

Conventional and RF/FS preservation experiments were repeated three times per cell type and/or condition that were examined. From each experiment, two to three samples were cut perpendicular to the growth plane into multiple 80-nm sections using a Reichert UCT ultramicrotome. Sections were stained with uranyl acetate followed by lead citrate using a Leica EMStainer. Sections were observed at 80 Kv using a JEOL 1200EX transmission electron microscope. Among the sections that were observed, we discarded sections in which the EC monolayer was not intact, the EC surface GCX was damaged or discontinuous, or freeze damage of the EC was observed. The occurrence of GCX loss and freeze damage, inherent but undesirable effects of handling the fragile GCX layer and

sometimes cryopreserving the cells below the critical rate of rapid freezing, limited the number of sample sections (n) to 1 to 3 per experiment, which is a total of at least 3 sections (n) per data set. Images of these sections were recorded on film. The negatives were scanned to create high resolution digital images. The contrast of all images was adjusted using Adobe Photoshop, and some images were grouped together to create panoramas using the Adobe Photoshop automated photo-merge feature. Images were later assessed for GCX presence, organization, and thickness. GCX thickness data sets were averaged, expressed as mean thickness ± SEM, and analyzed using a t-test with $P < 0.05$ indicating the statistical significance of the thickness of RF/FS-TEM processed BAEC GCX compared to the thickness of GCX on one of the following: BAEC processed by conventional TEM, RFPEC processed by RF/FS-TEM, BAEC cultured in the presence of heparinase, or BAEC culture in the absence of protein.

Immunoconfocal Microscropy

Previously described immunocytochemistry methods were used as the basis for the studies we conducted to confirm cell surface localization of the GCX[4, 9], with slight modifications. In brief, heparan sulfate (HS), hyaluronic acid (HA), and BSA GCX components were labeled on 2% paraformaldehyde/0.1% glutaraldehyde fixed EC. HS and HA were labeled with anti-HS (US Biologicals) and HA binding protein (Associates of Cape Cod), respectively. BSA was labeled with anti-BSA (Invitrogen Molecular Probes). 4′,6-diamidino-2-phenylindole (DAPI) marked the EC nucleii. Immunofluorescence was visualized with a Zeiss LSM 510 DUO confocal microscope, using a 60X objective at a zoom of 2. Z-stack images (planar sections collected 0.33 μm apart), 3D reconstructions, and cross-sectional cuts were performed using Zeiss LSM software. Using the cross-section images, HS, HA, and BSA thicknesses were measured per individual EC in the region overlying the center of the cell nucleus, but only when the EC surface GCX was continuous in that cell. Maximum HS, HA, and BSA thicknesses in each cross-section were also measured, as well as HS, HA, BSA thicknesses at cell-cell junctions. Each GCX thickness data set was generated from at least 3 cells or cell-cell junctions (n), averaged, expressed as mean thickness ± SEM, and analyzed using ANOVA.

RESULTS & DISCUSSION

In conventional TEM studies in which EC have been subjected to alcohol dehydration leading to the collapse of normally hydrated structures, GCX thickness has been found to be on the order of tens of nanometers[7, 10]. We repeated these conventional TEM experiments to compare the data to the results of our RF/FS-TEM studies. When BAEC were preserved by paraformaldehyde/glutaraldehyde fixation, dehydrated with alcohol, stained with ruthenium red, treated with a post-fixative containing osmium tetroxide contrast agent, and examined by TEM, the endothelial monolayer was found to be intact (figure 1A). All intercellular structures could be distinguished and the structures were found to be well preserved (figure 1C). A ruthenium red and osmium tetroxide positive extracellular layer, 41.68 ± 3.49 nm thick, was observed on the apical surface of the cells (figure 1C), with a few GCX strands extending 150 to 200 nm from the cell surface (figure 1C). Similar results were reported by Luft[15] who performed the first TEM study of ruthenium red stained GCX on explanted vascular tissue that underwent alcohol dehydration. Our conventional TEM findings also corroborate results of the *in vitro* TEM study of dehydrated, ruthenium red stained BAEC GCX reported by Ueda et al.[10] and the recent TEM study by Chappell et al.[7] who utilized lanthanum staining in place of ruthenium red to view GCX on dehydrated BAEC and human umbilical vein EC (HUVEC). Lanthanum binds to negatively charged glycoprotein[27] in a similar fashion as ruthenium red, but Lanthanum also stabilizes the GCX[28]. Therefore, it is reasonable to expect lanthanum-labeled GCX to be thicker than ruthenium red stained GCX.

The fact that a thicker GCX was not reported by Chappell et al.[7], even with the use of lanthanum, is difficult to explain but may be due to the sensitivity of endothelial cells *in vitro* to cell culture and electron microscopy methods.

GCX visualized by RF/FS-TEM was 100-fold thicker than the conventional TEM measurements. After EC were rapidly slam frozen and freeze substituted in acetone containing osmium tetroxide to avoid dehydration and collapse of hydrated cellular structures, when viewed by TEM the cell monolayer exhibited no damage (figure 1B). Membrane and individual organelles could be easily identified due to differences in affinity for osmium tetroxide (figures 1B and 1D). Cell structures were evenly distributed and classical in appearance, demonstrating successful preservation of cell morphology by slam freezing. Attached to the cell membrane and extending into the luminal and abluminal extracellular space, we could observe osmium tetroxide positive material, which was taken to be GCX. Morphologically, RF/FS preserved BAEC luminal GCX had the appearance of a fibril mesh unlike the shrub-like appearance of conventionally preserved *in vivo* GCX structures (e.g., van den Berg et al.[29]), a result of using RF/FS cryofixation in place of conventional chemical fixation[30]. Ameye et al. showed that chemical fixation of the cuticles of the pedicelleria primordial in the sea urchin *Paracentrotus lividus* and of the tube foot disc in the sea star *Asterias rubens* results in the preservation of a proteoglycan coat consisting of an accumulation (shrub) of very electron-dense material, while rapid cryofixation and freeze substitution preserves a proteoglycan coat made up of a loose meshwork of delicate fibrils.[30] In a similar fashion, the type of fixation used may explain the difference between the periodic structure of the GCX that has drawn much attention in previous studies (e.g., van den Berg et al. [29]) and the mesh structure of the GCX that we observed in our investigation. We particularly noted that RF/FS preserved BAEC GCX was less dense, more porous, and exhibited many elongated elements when compared to its conventionally preserved *in vitro* counterpart. The morphology and thickness of the glycocalyx varied spatially along the cell surface. It is particularly clear in figure 1B for BAEC that there were areas of the GCX in which elongated structures emanating from the cell surface were prominent; there were areas in which the elongated structures extended out to only about half the thickness of the GCX; and there were areas where there were no elongated structures at all. In locations where there were no elongated structures, the GCX layer had a distinct, more amorphous appearance that extended to the outer boundary of the GCX. The RF/FS-TEM processed GCX was 11.35 ± 0.21 μm thick (ranging from 10.8 to 12.5 μm) on BAEC (figure 1D). This ~11 μm BAEC GCX thickness is much greater than values derived from *in vitro* conventional TEM studies conducted by us (figures 1A and 1C) and others[10]. However, the RF/FS preserved BAEC GCX thickness that we report is comparable to the results of a recent study by Broekhuizen et al[14], who estimated a GCX thickness of 8.9 μm in vessels greater than 90 μm in diameter in live humans using sidestream dark field imaging and a fluorescent plasma tracer which was sterically excluded by the GCX.

When we applied RF/FS-TEM to assess the GCX on RFPEC, its morphology was that of a mesh (Figure 2B), similar to the morphology of RF/FS preserved BAEC GCX (Figure 2A), but denser and more amorphous with fewer distinguishable elongated elements. Morphological differences between endothelial cells of different vascular origin are well documented by several previously reported electron microscopy studies (reviewed by Tse and Stan[31]). The distinct morphology that we observed in RFPEC GCX is at least superficially, consistent with its microvascular function in the regulation of transendothelial permeability. In addition, we also found by RF/FS-TEM that RFPEC GCX was 5.83 ± 1.13 μm thick (ranging from 3.6 to 6.7 microns) (figure 2B), which is about half the thickness of BAEC GCX, showing that RF/FS-TEM can detect thickness variations due to different cell origins. The *in vitro* RFPEC GCX thickness we report is consistent with the previous *in vivo*

study by Megens et al.[16] and *ex vivo* study by van den Berg et al.[18] who imaged a 4.5-μm thick glycocalyx using two-photon and confocal laser scanning microscopy, respectively. In these studies in which mouse carotid arteries were examined, the endothelium was not dehydrated prior to obtaining thickness measurements, similar to our studies.

It is well-established that the components of the hydrated GCX include membrane-bound proteoglycans, glycosaminoglycans, and glycoproteins along with plasma proteins that bind to this structure [32, 33]. We expected that the GCX would be reduced in thickness after the addition of heparinase to EC culture media to partially remove membrane-bound heparan sulfate, based on a previous report of the effects of heparinase[34] and another GCX degrading enzyme, hyaluronidase[29], which cleaves membrane-bound hyaluronic acid. The previous studies of the effects of heparinase and hyaluronidase treatment on GCX thickness were performed *in vivo* and using vessels perfused with high concentrations of enzyme (50 U/mL of heparinase and 3000 to 15000 U/mL of hyaluronidase, where U is Sigma Units) dissolved in buffer that, in some cases, contained no BSA to stabilize the GCX [29, 34]. We conducted our study in a different manner, by investigating the influence of 15 mU/mL of heparinase treatment (this concentration blocks mechanotransduction events[1-5] and has less drastic effects on the GCX) on RF/FS processed BAEC that were cultured *in vitro* and under static conditions, and we did not observe changes in GCX thickness but modifications in its ultrastructure (figure 2C). Heparinase treated RF/FS preserved BAEC GCX was less dense and exhibited more elongated elements in the inner region closest to the plasma membrane (figure 2C) than its untreated counterpart (figure 2A). In our investigation, the effects of removing other physiologically and functionally relevant membrane-bound GCX components (CS, HA, glypican-1, and syndecans-1, -2, and -4) were not examined. To fully identify the nature of the components that make up the GCX mesh in RF/FS preserved EC, further studies of the dose-dependent effects of heparinase and other glycosaminoglycan degradation enzymes as well as systematic RNA inhibition of known proteoglycans are required.

When we studied the contribution of adsorbed protein to GCX thickness, by removal of FBS and BSA from EC culture media, BAEC (figure 2D) and RFPEC (not shown) GCX thickness was severely reduced to a level that was not visible by RF/FS-TEM, even at the same high magnification that permitted us to see the collapsed conventional TEM processed GCX shown in figure 1C. Our findings corroborate a previous report that the absence of plasma proteins collapses frog mesenteric capillary GCX[24]. In our study, protein removal did not simply collapse the GCX, but lead to its complete absence. This apparent shedding of the GCX is possibly due to the fact that without protein in its microenvironment the GCX is destabilized and strips away prior to or during the RF/FS process. The fact that substantial GCX was observed on EC grown in the presence of protein (figure 2A) and no GCX could be found on EC cultured in the absence of protein (figure 2D) provides a strong reminder of the importance of maintaining sufficient protein content in EC culture to sustain the GCX, allowing for proper assessment of GCX-mediated EC functions such as mechanotransduction. This result of protein removal on the GCX, taken together with the effect of heparinase treatment on the GCX, suggests the effectiveness of using RF/FS-TEM to reveal GCX modifications in response to micro-environmental changes such as protein content modification and enzymatic activity.

RF/FS-TEM has several advantages for observing hydrated, multicomponent structures such as the GCX, as outlined above. However, there are limitations. For example, while RF/FS-TEM reveals that *in vitro* GCX thickness extends to 5 microns for microvascular GCX and 11 microns for macrovascular GCX, no evidence is provided to suggest that these are the dimensions of the micro- and macro-vascular GCX *in vivo*. In the future, we plan to examine *in vivo* GCX ultrastructure in RF/FS preserved and TEM visualized tissue explanted from

murine blood vessels. In addition, experiments targeted at studying the mechanisms by which the GCX undergoes marked degradation at sites of platelet- or white blood cell-endothelial cell adhesion[42, 43] are accessible using the RF/FS TEM approach and cultured EC incubated with platelets or white blood cells. Ideally, addressing the question of GCX thickness *in vivo* using the RF/FS-TEM approach would best be accomplished if endothelial cells or vascular tissue were rapidly frozen *in situ* under fluid flow conditions and in the presence of circulating cells. This is technically not feasible at present.

A second limitation of RF/FS-TEM is that post-RF/FS immunogold labeling techniques adversely affect cell morphology and pre-RF/FS use of traditional immunogold or novel immunonanogold/silver enhancement labeling cause ice damage and subsequent loss of the GCX and other cellular structures (Ebong, Macaluso, Spray, and Tarbell, unpublished observations). To overcome this constraint, immunoconfocal microscopy was used to supplement RF/FS-TEM data, revealing the localization of individual GCX components, although with limited spatial resolution. Immunoconfocal studies of the GCX uncovered abundant HS, HA, and BSA on EC *in vitro*. BAEC and RFPEC exhibit HS, HA, and BSA layers of nonuniform thickness, ranging from ~1.4 μm to ~4.3 μm (figure 4). Prior to this work, similar thicknesses were reported *in vitro* by Barker et al.[6] and Stevens et al.[9]. While thickness differences are not statistically significant, BAEC HA (figure 4B) extends farther from the cell surface than BAEC HS (figure 4A), and RFPEC HA (figure 4E) appears to be confined to a region closer to the plasma membrane than RFPEC HS (figure 4D). The layer of BSA seen on BAEC and RFPEC (Figures 4C and 4F) is comparable in thickness to the HS and HA layers, demonstrating that the adsorbed protein is well integrated into the structure of the glycocalyx. Unfortunately, because immunoconfocal microscopy has limited spatial resolution and due to glare from the fluorescent labels, it would be difficult to use this technique to generate a detailed ultrastructural map of the GCX and its components. As such, we are currently developing a working immunogold labeling protocol for RF/FS TEM.

Our RF/FS-TEM measurements of GCX thickness (reaching 11 μm for BAEC and 6 μm for RFPEC) are significantly greater than our confocal immunolabeling measurements (4 μm maximum for BAEC and 3 μm maximum for RFPEC). This discrepancy is best explained by comparing the effects of RF/FS fixation for TEM to the effects of paraformaldehyde and glutaraldehyde fixation for confocal microscopy. While the RF/FS preserved GCX well represents the GCX of live cells[36], the paraformaldehyde/glutaraldehyde preserved GCX is distorted due to aldehyde-induced cross-linking of GCX components and subsequent pulling of the GCX inward towards the cell surface[37]. Notably, when compared to the aldehyde preserved configuration, the conventionally studied aldehyde fixed and dehydrated GCX least resembles the live structure (Figure 5)[37]. Our RF/FS TEM and immunoconfocal microscopy studies, taken together, provide a new life-like perspective of the GCX as a fibril mesh with well integrated components and substantial thickness.

The GCX thicknesses measured by RF/FS-TEM and immunoconfocal microscopy far exceed the estimated thickness that was recently reported by Potter and Damiano[8] and Potter et al.[38] who claimed that a significant GCX is not present *in vitro*, based on their particle tracking measurements in the near wall region. Despite the fact that these authors examined cultured EC that were not subjected to alcohol dehydration that would lead to GCX collapse, they exposed EC to other factors that might explain the altered GCX structure. Live BAEC or HUVEC were grown inside 100 – 150 μm collagen channels. Most *in vitro* experiments have been conducted on glass or plastic coated with fibronectin, not collagen, which may contribute to changes in GCX structure. In addition, EC-lined channels were perfused with media supplemented with a high concentration (4%) of 70 kDa Dextran, to raise the flow viscosity and minimize media consumption. The non-conventional Dextran use may have been problematical, as it has been shown to be sterically excluded from the GCX[20]. Rather

than being incorporated into the GCX and contributing to the stabilization and enhancement of its thickness, as do other components of the media, the dextran increases the viscosity of the core flow and may lead to deformation, compression, or shedding of the glycocalyx. Microscopy experiments and antibody or lectin staining would be required to verify the presence of a GCX and confirm that the Dextran in the media does not alter GCX structure when compared to normal media.

In summary, we have shown that, compared to conventional methods, RF/FS-TEM provides high resolution detection of the EC GCX *in vitro*. RF/FS-TEM allows for the maintenance of hydration needed to stabilize hydrophilic cellular structures after cell preservation. The use of RF/FS-TEM makes it possible to detect small structural alterations, as we have shown by comparing cell types and culture environment. We hope that this work clarifies much of the ambiguity surrounding the existence of EC GCX *in vitro*. The cell culture model continues to play an important role in fundamental studies of the relationship between the GCX and endothelial mechanotransduction, other physiological processes, and vascular disease.

Acknowledgments

We acknowledge the Albert Einstein College of Medicine (AECOM) Analytical Imaging Facility (AIF) for assistance with the TEM studies, recognizing the contributions of AIF personnel Leslie Gunther-Cummins, Hillary Guzik, Geoffrey Perumal, and Juan Jimenez. We also thank Dr. Kostantin Dobrenis and the AECOM Cellular and Molecular Neuroimaging Core for making the confocal microscope available to us. Our gratitude is also extended to Drs. David Hall and Mia Thi for proof-reading and discussion of the manuscript.

SOURCES OF FUNDING This work was supported by the National Institutes of Health Grants 5T32HL007675, HL73732, HL57093, and HL094889.

REFERENCES

1. Florian JA, Kosky JR, Ainslie K, Pang Z, Dull RO, Tarbell JM. Heparan sulfate proteoglycan is a mechanosensor on endothelial cells. Circ Res. 2003; 93:e136–142. [PubMed: 14563712]
2. Pahakis MY, Kosky JR, Dull RO, Tarbell JM. The role of endothelial glycocalyx components in mechanotransduction of fluid shear stress. Biochem Biophys Res Commun. 2007; 355:228–233. [PubMed: 17291452]
3. Lopez-Quintero SV, Amaya R, Pahakis M, Tarbell JM. The endothelial glycocalyx mediates shear-induced changes in hydraulic conductivity. Am J Physiol Heart Circ Physiol. 2009; 296:H1451–1456. [PubMed: 19286951]
4. Thi MM, Tarbell JM, Weinbaum S, Spray DC. The role of the glycocalyx in reorganization of the actin cytoskeleton under fluid shear stress: a “bumper-car” model. Proc Natl Acad Sci U S A. 2004; 101:16483–16488. [PubMed: 15545600]
5. Yao Y, Rabodzey A, Dewey CF Jr. Glycocalyx modulates the motility and proliferative response of vascular endothelium to fluid shear stress. Am J Physiol Heart Circ Physiol. 2007; 293:H1023–1030. [PubMed: 17468337]
6. Barker AL, Konopatskaya O, Neal CR, Macpherson JV, Whatmore JL, Winlove CP, Unwin PR, Shore AC. Observation and characterisation of the glycocalyx of viable human endothelial cells using confocal laser scanning microscopy. Physical chemistry chemical physics. 2004; 6:1006–1011.
7. Chappell D, Jacob M, Paul O, Rehm M, Welsch U, Stoeckelhuber M, Conzen P, Becker BF. The glycocalyx of the human umbilical vein endothelial cell: an impressive structure ex vivo but not in culture. Circ Res. 2009; 104:1313–1317. [PubMed: 19423849]
8. Potter DR, Damiano ER. The hydrodynamically relevant endothelial cell glycocalyx observed in vivo is absent in vitro. Circ Res. 2008; 102:770–776. [PubMed: 18258858]

9. Stevens AP, Hlady V, Dull RO. Fluorescence correlation spectroscopy can probe albumin dynamics inside lung endothelial glycocalyx. Am J Physiol Lung Cell Mol Physiol. 2007; 293:L328–335. [PubMed: 17483194]
10. Ueda A, Shimomura M, Ikeda M, Yamaguchi R, Tanishita K. Effect of glycocalyx on shear-dependent albumin uptake in endothelial cells. Am J Physiol Heart Circ Physiol. 2004; 287:H2287–2294. [PubMed: 15256377]
11. Janczyk P, Hansen S, Bahramsoltani M, Plendl J. The glycocalyx of human, bovine and murine microvascular endothelial cells cultured in vitro. J Electron Microsc (Tokyo). 2010; 59:291–298. [PubMed: 20304776]
12. Devaraj S, Yun JM, Adamson G, Galvez J, Jialal I. C-reactive protein impairs the endothelial glycocalyx resulting in endothelial dysfunction. Cardiovasc Res. 2009; 84:479–484. [PubMed: 19620133]
13. Singh A, Satchell SC, Neal CR, McKenzie EA, Tooke JE, Mathieson PW. Glomerular endothelial glycocalyx constitutes a barrier to protein permeability. J Am Soc Nephrol. 2007; 18:2885–2893. [PubMed: 17942961]
14. Broekhuizen LN, Lemkes BA, Mooij HL, Meuwese MC, Verberne H, Holleman F, Schlingemann RO, Nieuwdorp M, Stroes ES, Vink H. Effect of sulodexide on endothelial glycocalyx and vascular permeability in patients with type 2 diabetes mellitus. Diabetologia. 2010; 53:2646–2655. [PubMed: 20865240]
15. Luft JH. Fine structures of capillary and endocapillary layer as revealed by ruthenium red. Fed Proc. 1966; 25:1773–1783. [PubMed: 5927412]
16. Megens RT, Reitsma S, Schiffers PH, Hilgers RH, De Mey JG, Slaaf DW, oude Egbrink MG, van Zandvoort MA. Two-photon microscopy of vital murine elastic and muscular arteries. Combined structural and functional imaging with subcellular resolution. J Vasc Res. 2007; 44:87–98. [PubMed: 17192719]
17. Rostgaard J, Qvortrup K. Electron microscopic demonstrations of filamentous molecular sieve plugs in capillary fenestrae. Microvasc Res. 1997; 53:1–13. [PubMed: 9056471]
18. van den Berg BM, Spaan JA, Vink H. Impaired glycocalyx barrier properties contribute to enhanced intimal low-density lipoprotein accumulation at the carotid artery bifurcation in mice. Pflugers Arch. 2009; 457:1199–1206. [PubMed: 18839207]
19. van Haaren PM, VanBavel E, Vink H, Spaan JA. Localization of the permeability barrier to solutes in isolated arteries by confocal microscopy. Am J Physiol Heart Circ Physiol. 2003; 285:H2848–2856. [PubMed: 12907418]
20. Vink H, Duling BR. Identification of distinct luminal domains for macromolecules, erythrocytes, and leukocytes within mammalian capillaries. Circ Res. 1996; 79:581–589. [PubMed: 8781491]
21. Dalen H, Lieberman M, LeFurgey A, Scheie P, Sommer JR. Quick-freezing of cultured cardiac cells in situ with special attention to the mitochondrial ultrastructure. J Microsc. 1992; 168:259–273. [PubMed: 1484378]
22. von Schack ML, Fakan S, Villiger W, Muller M. Cryofixation and cryosubstitution: a useful alternative in the analyses of cellular fine structure. Eur J Histochem. 1993; 37:5–18. [PubMed: 7682867]
23. Bhat SN, Sharma A, Bhat SV. Vitrification and glass transition of water: insights from spin probe ESR. Phys Rev Lett. 2005; 95:235702. [PubMed: 16384318]
24. Adamson RH, Clough G. Plasma proteins modify the endothelial cell glycocalyx of frog mesenteric microvessels. J Physiol. 1992; 445:473–486. [PubMed: 1501143]
25. Marcum JA, Rosenberg RD. Heparinlike molecules with anticoagulant activity are synthesized by cultured endothelial cells. Biochem Biophys Res Commun. 1985; 126:365–372. [PubMed: 3970699]
26. Wagner RC, Kreiner P, Barrnett RJ, Bitensky MW. Biochemical characterization and cytochemical localization of a catecholamine-sensitive adenylate cyclase in isolated capillary endothelium. Proc Natl Acad Sci U S A. 1972; 69:3175–3179. [PubMed: 4564206]
27. Bozzola JJ, Polakoski K, Haas N, Russell LD, Campbell P, Peterson RN. Localization of boar sperm proacrosin during spermatogenesis and during sperm maturation in the epididymis. Am J Anat. 1991; 192:129–141. [PubMed: 1759680]

28. Jacob M, Rehm M, Loetsch M, Paul JO, Bruegger D, Welsch U, Conzen P, Becker BF. The endothelial glycocalyx prefers albumin for evoking shear stress-induced, nitric oxide-mediated coronary dilatation. J Vasc Res. 2007; 44:435–443. [PubMed: 17622736]
29. van den Berg BM, Vink H, Spaan JA. The endothelial glycocalyx protects against myocardial edema. Circ Res. 2003; 92:592–594. [PubMed: 12637366]
30. Ameye L, Hermann R, DuBois P, Flammang P. Ultrastructure of the echinoderm cuticle after fast-freezing/freeze substitution and conventional chemical fixations. Microsc Res Tech. 2000; 48:385–393. [PubMed: 10738319]
31. Tse D, Stan RV. Morphological heterogeneity of endothelium. Semin Thromb Hemost. 2010; 36:236–245. [PubMed: 20490976]
32. Tarbell JM, Pahakis MY. Mechanotransduction and the glycocalyx. J Intern Med. 2006; 259:339–350. [PubMed: 16594902]
33. Pries AR, Secomb TW, Gaehtgens P. The endothelial surface layer. Pflugers Arch. 2000; 440:653–666. [PubMed: 11007304]
34. Gao L, Lipowsky HH. Composition of the endothelial glycocalyx and its relation to its thickness and diffusion of small solutes. Microvasc Res. 2010; 80:394–401. [PubMed: 20600162]
35. Han Y, Weinbaum S, Spaan JA, Vink H. Large-deformation analysis of the elastic recoil of fiber layers in a Brinkman medium with application to the endothelial glycocalyx. J Fluid Mech. 2006; 554:217–235.
36. Ladinsky MS. Micromanipulator-assisted vitreous cryosectioning and sample preparation by high-pressure freezing. Methods Enzymol. 481:165–194. [PubMed: 20887858]
37. Heuser J. Whatever happened to the ‘microtrabecular concept’? Biol Cell. 2002; 94:561–596. [PubMed: 12732437]
38. Potter DR, Jiang J, Damiano ER. The recovery time course of the endothelial cell glycocalyx in vivo and its implications in vitro. Circ Res. 2009; 104:1318–1325. [PubMed: 19443840]
39. Lewis JC, Taylor RG, Jones ND, St Clair RW, Cornhill JF. Endothelial surface characteristics in pigeon coronary artery atherosclerosis. I. Cellular alterations during the initial stages of dietary cholesterol challenge. Lab Invest. 1982; 46:123–138. [PubMed: 7062718]
40. Vink H, Constantinescu AA, Spaan JA. Oxidized lipoproteins degrade the endothelial surface layer: implications for platelet-endothelial cell adhesion. Circulation. 2000; 101:1500–1502. [PubMed: 10747340]
41. van den Berg BM, Spaan JA, Rolf TM, Vink H. Atherogenic region and diet diminish glycocalyx dimension and increase intima-to-media ratios at murine carotid artery bifurcation. Am J Physiol Heart Circ Physiol. 2006; 290:H915–920. [PubMed: 16155109]
42. Kumase F, Morizane Y, Mohri S, Takasu I, Ohtsuka A, Ohtsuki H. Glycocalyx degradation in retinal and choroidal capillary endothelium in rats with diabetes and hypertension. Acta Med Okayama. 2010; 64:277–283. [PubMed: 20975760]
43. Chappell D, Dorfler N, Jacob M, Rehm M, Welsch U, Conzen P, Becker BF. Glycocalyx protection reduces leukocyte adhesion after ischemia/reperfusion. Shock. 2010; 34:133–139. [PubMed: 20634656]

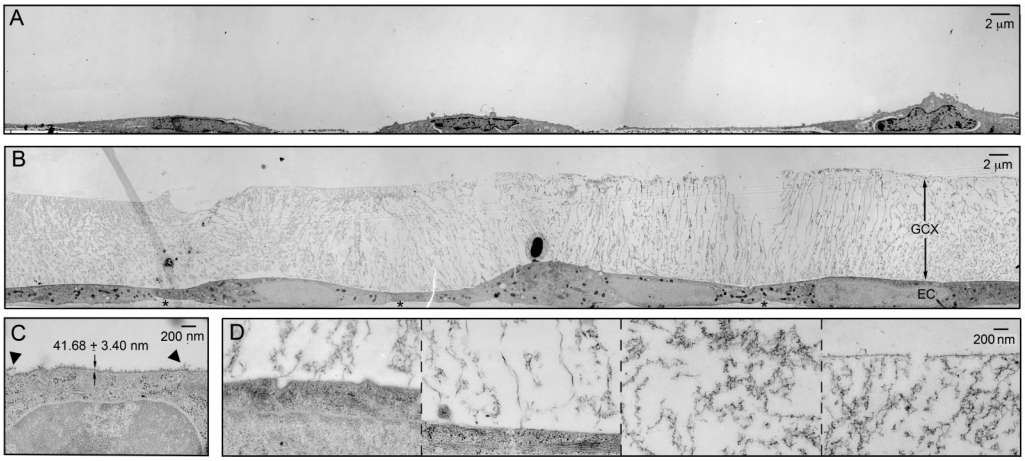

Figure 1.

TEM of GCX-covered BAEC (A) preserved conventionally, labeled with ruthenium red and osmium tetroxide, and alcohol dehydrated, or (B) preserved by RF/FS and osmium tetroxide stained (stars (*) denote abluminal GCX). (C) High magnification image of conventionally preserved BAEC GCX (arrowheads (▼) denote extended strands of GCX). (D) High magnification image of RF/FS preserved BAEC GCX, showing (from left to right) locations near the cell membrane, further away from the cell membrane, in the center region of the GCX, and at the most apical surface of the GCX .

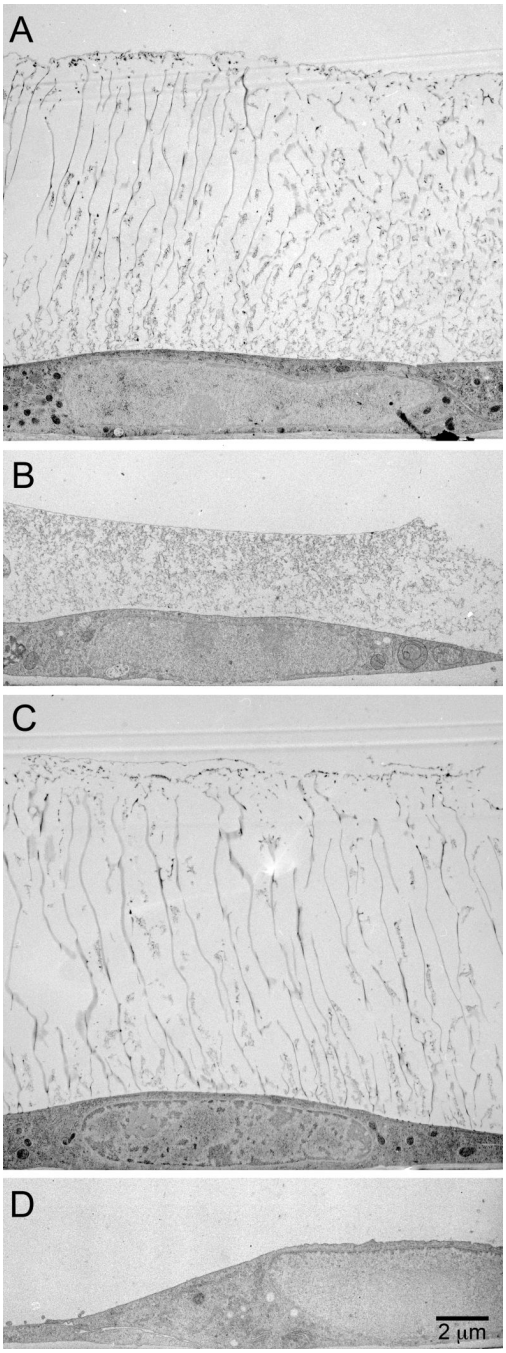

Figure 2.
RF/FS preservation, osmium tetroxide staining, and TEM of (A) untreated BAEC GCX, (B) untreated RFPEC GCX, (C) BAEC GCX treated with Heparanase III to degrade the heparan sulfate component of the GCX, and (D) GCX of BAEC cultured in the absence of FBS and BSA.

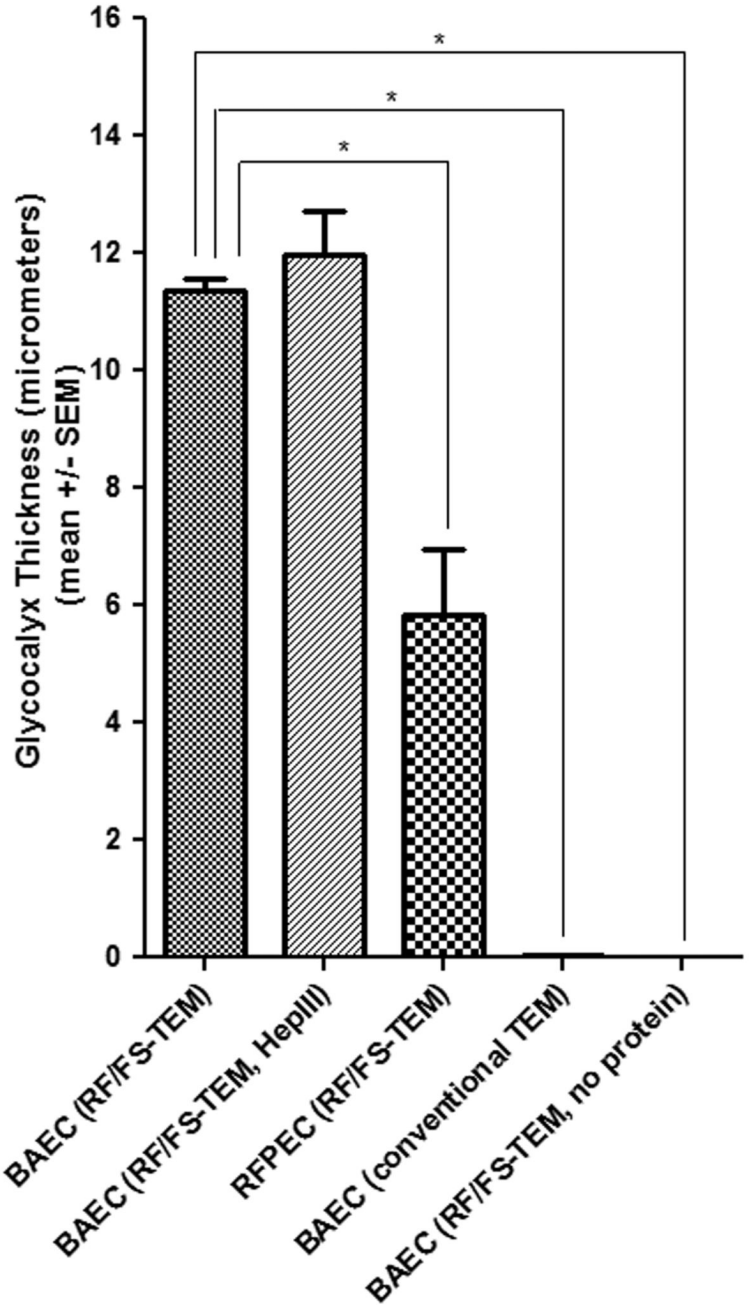

Figure 3.

The GCX thickness measurements, differences between thicknesses of various cell types and/or treatments, standard errors, and statistical analysis demonstrate the validity and stability of the RF/FS TEM approach. BAEC GCX thickness was 11.35 ± 0.21 μm (n = 7 sections) with RF/FS-TEM, but 0.042 ± 0.003 μm (n = 3 sections) with conventional-TEM. 5.83 ± 1.13 μm (n = 3 sections) RFPEC GCX thickness was determined by RF/FS-TEM. BAEC GCX was 11.98 ± 0.73 μm (n = 4 sections) with heparinase III treatment and undetectable without protein. *P < 0.05.

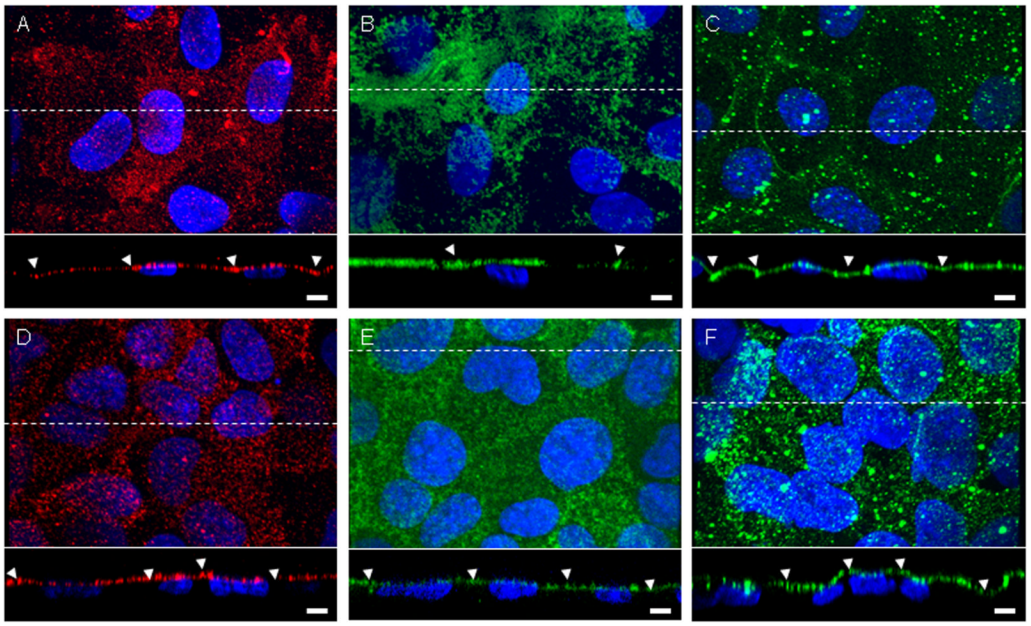

G

		GCX Layer Thickness (μm ± SEM)		
		Average	*Maximum*	*Junctional*
BAEC	*HS*	1.38 ± 0.07 (n = 8)	1.41 ± 0.12 (n = 4)	1.75 ± 0.14 (n = 3)
	HA	2.08 ± 0.26 (n = 8)	4.29 ± 1.05 (n = 7)	3.00 ± 0.54 (n = 7)
	BSA	1.47 ± 0.15 (n = 23)	2.74 ± 0.24 (n = 7)	1.33 ± 0.09 (n = 21)
RFPEC	*HS*	2.00 ± 0.13 (n = 15)	2.41 ± 0.08 (n = 3)	3.08 ± 0.51 (n = 3)
	HA	1.85 ± 0.10 (n = 12)	1.87 ± 0.37 (n = 4)	2.12 ± 0.25 (n = 4)
	BSA	1.53 ± 0.11 (n = 19)	2.68 ± 0.12 (n = 6)	1.48 ± 0.10 (n = 16)

Note: Statistics were performed to determine significant differences ($P < 0.05$) between the average thicknesses of the HS, HA, and BSA layers (maximum and junctional thickness data were not analyzed). The three layers were not found to be statistically significantly different in thickness.

Figure 4.

Confocal micrographs of EC HS (red), HA (green), BSA (green), and nucleii (blue). (A) BAEC HS, (B) BAEC HA, (C) BAEC BSA, (D) RFPEC HS, (E) RFPEC HA, and (F) RFPEC BSA are shown. Bar = 5 um. (G) Average ± SEM GCX thickness (n = GCX-covered EC nucleii), maximum GCX thickness per cross-section, and junctional GCX thickness. Arrowheads: locations of cell-to-cell junctions.

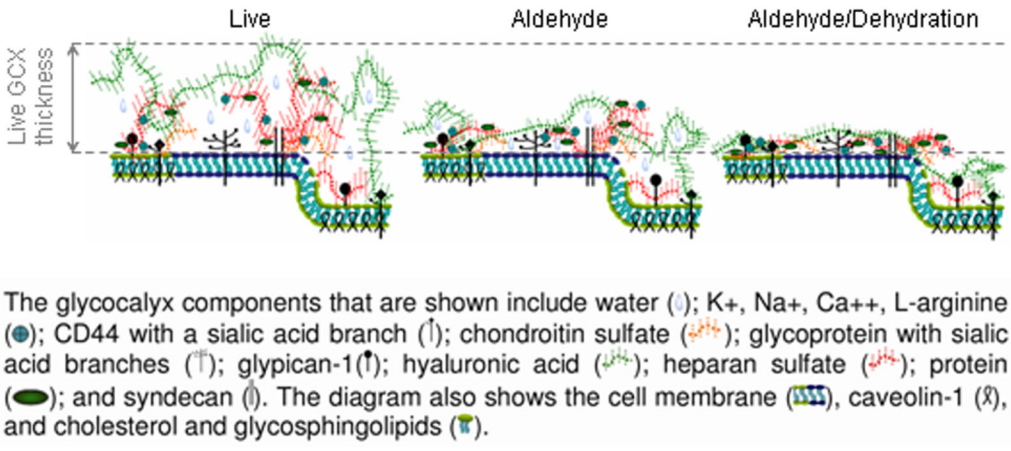

Figure 5.
This cartoon, redrawn from Pahakis et al.[2] on the basis of Heuser's review[37], depicts how live conditions, aldehyde fixation, and aldehyde combined with dehydration differentially affect GCX thickness and ultrastructural composition.

Table 1

Selected publications of GCX thickness measurements.

Setting	Microscopic Visualization	GCX Fixation	GCX Marker	Species and Vessel/Cell Type	GCX Thickness (μm)	Reference
In Vivo* and *Ex Vivo	TEM	Glut	RR	Mouse diaphragmatic capillary	0.02	Luft (1966)[15]
	TEM	Glut	Fluorocarbon	Rat capillary	0.05 to 0.10	Rostgaard and Qvortrup (1997)[17]
	IM	No fixation	FITC dextran-labeled plasma	Hamster muscle capillary[a]	0.40 to 0.50	Vink and Duling (1996)[20]
	μ-PIV	No Fixation	Flourescent microspheres in saline	Mouse cremaster venules[c]	0.50	Potter and Damiano (2008)[8]
	TEM	Glut/PFA	Alcian Blue and Lanthanum	Rat aorta	0.53	Devaraj et al. (2009)[12]
	TEM	Glut	Lanthanum	Human umbilical vein	0.80	Chappell et al. (2009)[7]
	IM	No fixation	FITC dextran-labeled plasma	Rat small arteries[b]	2.00 to 3.00	van Haaren et al. (2003)[19]
	TPLSM	No fixation	WGA-FITC	Mouse carotid arteries	4.50	Megens et al. (2007)[16]
	CLSM	No fixation	HABP-AF555 and AF488 tagged anti-HS	Mouse carotid arteries	2.20 to 4.30	van den Berg et al. (2009)[18]
	SDF Imaging	No fixation	Fluorescein and indocyanine green	Human sublingual and retinal vessels[g]	8.90	Broekhuizen et al (2010)[14]
In Vitro	TEM	Glut	RR	MCMVEC	0.00 to 0.20	Janczyk et al. (2010)[11]
	TEM	Glut	RR	HDMVEC	0.01 to 0.02	Janczyk et al. (2010)[11]
	TEM	Glut	RR	BLMVEC	0.01 to 0.03	Janczyk et al. (2010)[11]
	μ-PIV	No Fixation	Flourescent mcrospheres in media	HUVEC[d]	0.03	Potter and Damiano (2008)[8]
	μ-PIV	No Fixation	Flourescent mcrospheres in media	BAEC[e]	0.02	Potter and Damiano (2008)[8]
	TEM	Glut	Lanthanum	HUVEC	0.03	Chappell et al. (2009)[7]
	TEM	Glut	RR	BAEC	0.02 to 0.04	Ueda et al. (2004)[10]
	TEM	Glut	Alcian Blue	CiGEnC	0.20	Singh et al. (2007)[13]
	TEM	Glut/PFA	Alcian Blue and Lanthanum	HAEC	0.85	Devaraj et al. (2009)[12]
	CLSM	PFA	Fluorescent anti-HS	RFPEC	2.00[f]	Thi et al. (2004)[4]
	CLSM	No Fixation	WGA-FITC	HUVEC	2.50	Barker et al. (2004)[6]
	CLSM	PFA	HABP-FITC and fluorescent anti-HS	BLMVEC	2.00 to 3.00	Stevens et al. (2007)[9]

TEM: transmission electron microscopy; Glut: glutaraldehyde; PFA: paraformaldehyde; RR: ruthenium red; IM: Intravital Microscopy; TPLSM: two-photon laser scanning microscopy; CLSM: confocal laser scanning miscroscopy; WGA: wheat germ agglutinin; SDF: sidestream dark field; FITC: fluorescein isothiocyanate; HABP: hyaluronic acid binding protein; AF555: Alexa Fluor 555; AF488: Alexa Fluor 488; μ-PIV: microparticle image velocimetry; HUVEC: human umbilical vein ECs; BAEC: bovine aortic ECs; BLMVEC: bovine lung microvascular ECs; HAEC: human aortic ECs; CiGEnC: conditionally immortalized human glomerular endothelial cells; MCMVEC: murine cardiac microvascular ECs; HDMVEC: human dermal microvascular ECs; BLMVEC: bovine luteal microvascular ECs; RFPEC: rat fat pad ECs.

[a] 5.1 ± 0.1 μm diameter

[b] 148 ± 5 μm diameter

[c] 45 ± 20 μm diameter

[d] Cells were plated in ~110 to 150 μm diameter collagen channels

[e] Cells were plated in ~88 to 109 μm diameter collagen channels

[f] GCX thickness was not reported in the publication, but was obtained in reference to the scale bar and relative to the cell dimensions.

[g] 90 μm diameter